

Long-range μ PIV in the turbulent region of a jet, at high Reynolds numbers

D. Fiscaletti¹, G.E. Elsinga¹, and J. Westerweel¹

¹Lab. for Aero & Hydrodynamics, Department of Mechanical Engineering, Delft University of Technology, Leeghwaterstraat 21 2628 CA Delft, The Netherlands, d.fiscaletti@tudelft.nl

ABSTRACT

The present work involves the investigation of the fine scale motions in the turbulent region of a high Reynolds number air jet. In the fully developed region of the jets, the small scales of turbulence are assumed to be isotropic, and expected to contain elongated vortices (worms), whose diameter scales with the Kolmogorov length scale. Aimed at capturing the worms, a long-range μ PIV system is developed. The main design parameters of the PIV experiment are set on the basis of a hot-wire characterization of the flow. Furthermore, a benchmark hot-wire acquisition allows a validation of the present μ PIV measurements, by comparison of the main statistics. In the implementation of the measurement technique, the low concentration of seeding particles and the short depth of focus represent both the main challenges. Eventually, instantaneous vector maps from PIV measurements are presented, where the dissipative small scale structures are resolved.

INTRODUCTION

The spatial organization of the small-scale motions plays a decisive role in the rate of dissipation of the turbulent kinetic energy, and thus, in the energy cascade mechanism. As a consequence, many works have focused on the behaviour of the viscous scales. In particular, the small scales seem to organize themselves in structures, shaped as elongated vortices (worms) [1]. The worm-like structures were originally identified from DNS datasets of isotropic turbulence. Their diameter was observed to scale with the Kolmogorov length scale, whereas their length with the integral length scale of the flow [2]. Recently, the advent of CMOS cameras allowed a 3D reconstruction of stereo-PIV data (cinematographic stereoscopic PIV). The technique was used to experimentally investigate the fully developed region of an air jet [3]. It was evidenced that the clustering of the vortex tubes induced the formation of regions of intense dissipation (sheets). Although this study established a connection between the 3D spatial organization of the small-scale structures and the dissipation of turbulent kinetic energy, the Reynolds number of the jet under analysis was relatively low. In the present study, the fine scale motions of a turbulent air jet were investigated at a high Reynolds number, where the productive and the dissipative scales present a separation of two decades in the power spectrum. In jets, the large scales depend on the geometry of the nozzle, whereas the size of the small scales is inversely proportional to the Reynolds number. Therefore, the resolution of the viscous scales in flows at a high Reynolds number requires the use of a microscope, in a long-range μ PIV system. The use of the technique is still very limited, and of recent introduction. One of its first successful application has been reported in 2002, when the dissipative turbulent structures in a water pipe flow could be resolved [4]. Later, the technique was proficiently applied to evaluate the wall-shear-stress in a turbulent boundary layer [5], and to investigate the laminar separation bubble above a helicopter blade tip [6].

The first objective of this work is to resolve the fine scale structures of turbulence in the 2D velocity vector maps, obtained from long-range μ PIV acquisitions. Moreover, μ PIV data should be compared to benchmark hot-wire results for sake of validation.

EXPERIMENTAL SETUP

The governing non-dimensional numbers of the jet at the nozzle, whose diameter is $D = 8 \text{ mm}$, can be estimated as $Re = 6.6 \cdot 10^4$ and $Ma = 0.37$. A nozzle speed of 124.8 m/s , used for the computation of the Reynolds number, comes from Pitot tube measurements. A first characterization of the jet with hot-wire anemometry (Figure 1) was aimed at estimating the size of the turbulence scales, at different distances from the nozzle. Details over the experimental dataset from hot-wire anemometry are available in [7]. From the following relationship, an estimate of the dissipation rate in jets is provided [8]:

$$\varepsilon \approx 0.015 \frac{U_c^3}{r_{1/2}} \quad (1)$$

where U_c is the centerline velocity and $r_{1/2}$ is the jet's half-width. Based on the dissipation rate, the size of the Kolmogorov scales can be calculated at the different locations. Along the centerline, at a downstream distance of $x/D = 70$, the Kolmogorov length scale is around $60 \mu\text{m}$. The following are some relevant length scales at the measurement location, obtained from hot-wire measurements: jet's half-width $r_{1/2} = 52 \text{ mm}$, Taylor micro-scale $\lambda = 2.15 \text{ mm}$, $Re_\lambda = 340$. The mentioned hot-wire measurements allowed to design the PIV experiment. The μ PIV system consists of a Nd:YAG laser (Quanta-Ray by Spectra-Physics), a 1k x 1.3k double shutter CCD-camera, and a long distance microscope. Figure 4 shows the μ PIV system. In the present setup, the Questar QM-1 is chosen as a long distance microscope, whose working distance ranges from 550 mm to 1560 mm . The same microscope had been already used to successfully measure the turbulence in a pipe flow [4]. In that work, structures sized in $200 \mu\text{m}$ were resolved, with a magnification factor of 2.6,

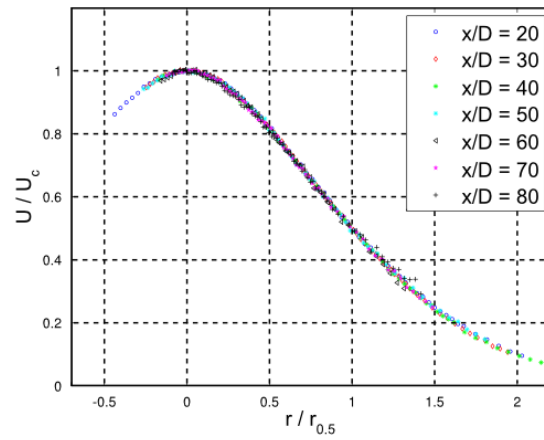


Figure 1: Profiles of the mean axial velocity of the air jet, measured with single probe hot-wire anemometry. The velocity profiles and the radial location were nondimensionalized by the mean centerline velocity, and by the jet's half width, respectively.

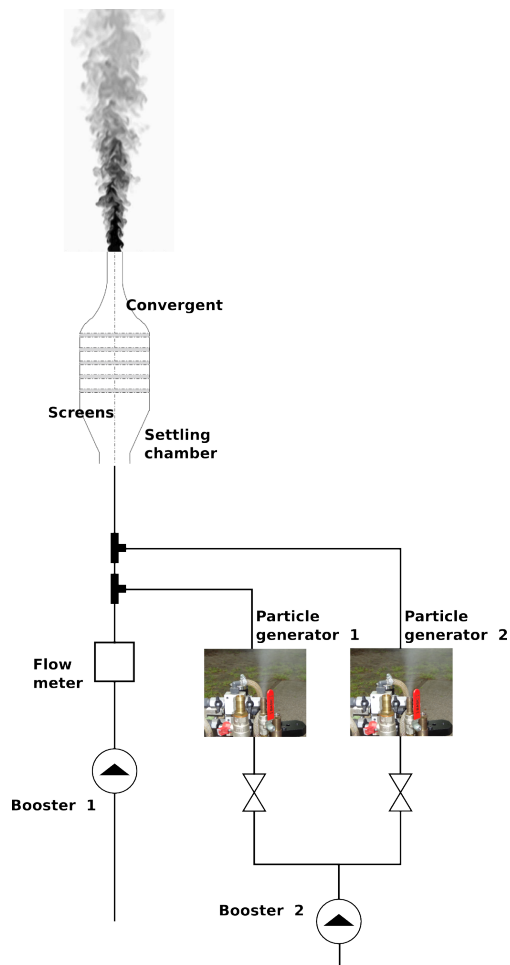


Figure 2: Sketch of the system for the supply of the seeded flow.

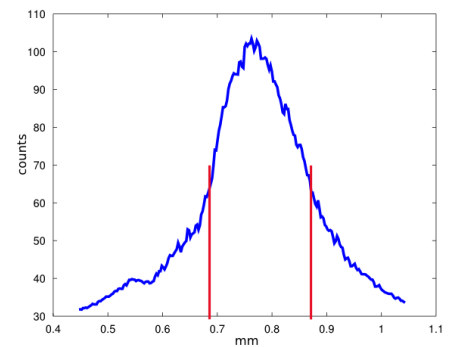
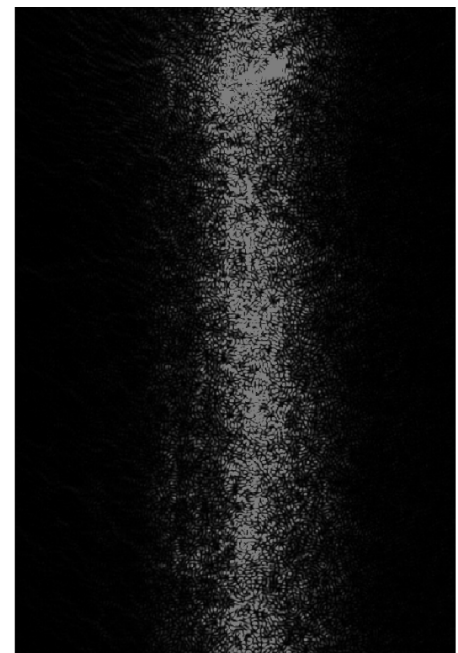


Figure 3: Top: recorded image of the laser sheet, as reflected by a plexi plate positioned at 45° with respect to the camera. Bottom: light intensity distribution for the estimate of the thickness of the light sheet.

and a working distance of 550 mm. As seeding tracers in the jet's flow, we used DEHS particles (Di(2-ethylhexyl)sebacate, sebacic acid), obtained with the Laskin nozzle. One of the most challenging aspects in the design of this sort of experiments is the achievement of a sufficient concentration of particle images within the field of view. This is intimately linked to the way the flow is seeded. From the analytical formulation of the mean velocity profile in round jets [9], the mass flow at 70 diameters downstream the jet nozzle is more than twenty times higher than at the centerline. This would suggest to seed the entraining ambient flow. On the other hand, the seeding of the whole ambient where the jet develops would create an optical barrier between the measurement domain and the microscope, therefore this option was deemed impractical. Instead, we decided to directly insert particles within the air jet. The injection of particles was done a couple of meters upstream the settling chamber of the jet, so to achieve a uniform concentration of tracer particles within the flow, and to avoid any perturbative effect that would result from introducing a nozzle into the flow. Two particle generators were used, pressurized at 2.2 bar by a compressor. Thus, the air jet under investigation was supplied by both the seeded flow, and the unseeded air flow from a second compressor, as sketched in Figure 2. From the manual of the particle generators (manufactured by PIVTEC GmbH), the particle size distribution of the tracers has a peak for a size of 1 μm . Based on a particle diameter of 1 μm , the response time of the seeding particles is computed to be 3 μs . On the other hand, the Kolmogorov time scale at the measurement location is $\tau_\eta = \sqrt{\nu/\varepsilon} = 200 \mu\text{s}$, therefore two orders of magnitude larger than the time response of the particles. This indicates that the velocity fluctuations in the flow can be tracked. The particle concentration of a PIV image is shown in Figure 5. Details over the settling chamber and the shape of the nozzle can be found in [10]. The magnification factor adopted was 2.5, with a working distance of 580 mm. Data were acquired at the frequency of 5 Hz, and the particle suction system was kept off during the measurement process. In μPIV , the depth of focus is shorter than in PIV. As a consequence, if the thickness of the light sheet is larger than the depth of focus,

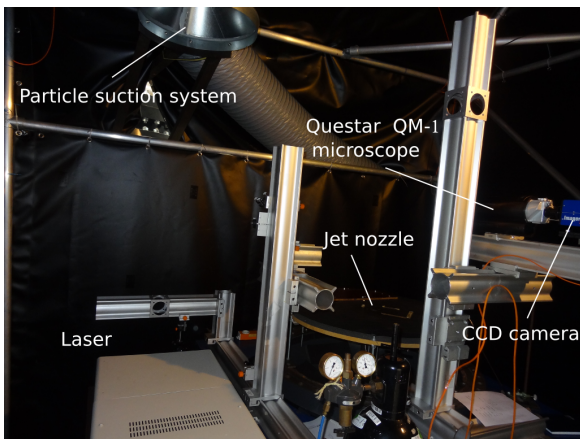


Figure 4: The experimental setup.

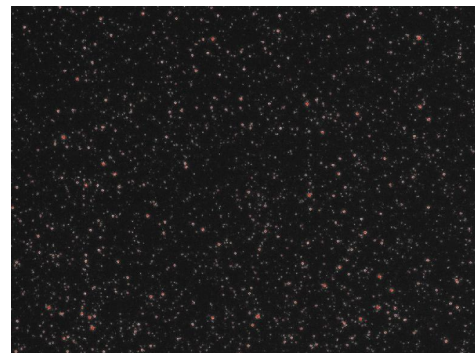


Figure 5: A μPIV image.

some out-of-focus particles could be illuminated, thus appearing in the shape of "donuts" [11]. The presence of out-of-focus particles in the pair of images is a source of error in the correlation process, and it should be avoided. Therefore, the thickness of the light sheet should match the depth of focus of the microscope. To attain this, a cylindrical lens was used to focus the light sheet within the measurement domain. In order to estimate the thickness, we recorded the laser light reflected on a plexi plate, positioned at around 45° with respect to the camera. The light intensity profile is almost gaussian. Assuming that the laser light can be considered visible on the camera at intensities higher than 50% of the peak value, the thickness of the light sheet is around 180 μm (Figure 3).

RESULTS AND DISCUSSION

The dataset of image pairs was processed through a cross-correlation algorithm, implemented in the software *DaViS* by *LaVision*. A two-pass refinement of the grid was adopted, with a final interrogation window of 64 x 64 pixel, and a 50% window overlap. The size of the interrogation window is 160 μm , thus almost equal to the thickness of the light sheet. A scheme for the detection of the spurious vectors was applied to the present set of data. A vector was considered a spurious one when its magnitude was outside a certain range, depending on the neighbouring vectors [11]. This range was represented by a deviation equal to 1.2 times the *rms* of the neighbouring vectors, applied to the median vector of the neighbours themselves. The outliers mainly concentrated at the edge of the vector map. The reason for that was a lack of correlation due to the finite size of the PIV image. After applying a masking to the vector map, aimed at removing those vectors, the percentage of good vectors was higher than 94% throughout the whole dataset. This high percentage of good vectors allowed the application of the algorithm for the replacement of the outliers, based on linear interpolation of the neighbours.

The μPIV set of data is composed of 6000 vector maps. This was validated by comparison with a hot-wire acquisition, at the same measurement location. An unseeded jet was supplied, which was intended to be measured by hot-wire. The two nozzle speeds of both the seeded (for PIV) and the unseeded (for hot-wire) jet matched each others, hence their Reynolds numbers. The main statistics of the flow, such as mean, rms, and skewness, were computed for both the datasets, and then nondimensionalized by the centerline velocity (10.6 m/s). In Table 1, the result of the comparison is given. The agreement between the results obtained in the two different measurement technique is remarkable, and validates the PIV results.

In Figures 6, 7, 8, 9, 10, 11, 12, and 13, a selection of instantaneous vector maps, each of those relative to the respective average velocity, is shown. The measurement technique is adequate to capture the dissipative structures, which scale with the Kolmogorov length scale. These structures, shaped as elongated vortices, should not present any preferential orientation. Instead, their axes are expected to be randomly positioned in the 3D space, after the assumption of isotropy of the small scales. The vortices we see might be the worm-like structures intersecting the plane of the light sheet. Unfortunately, planar PIV data do not allow any speculations over

Table 1: Comparison between the main statistics of the turbulent flow computed from single probe hot-wire measurements, and μ PIV results.

	HW	μ PIV
mean	0.841	0.837
rms	0.254	0.239
skewn.	0.02	0.01

the axial development of these vortical structures. In future investigations, another camera is going to be added to the PIV system, thus developing a stereoscopic configuration of the system.

Furthermore, even if the main goal of the present study is the resolution of the fine scale motions, the high Reynolds number of the flow under investigation represents an important element of novelty. As a consequence, the small scales are expected to be clearly separated from the large scales, which is an evidence of a fully-developed turbulence. In order to check the scale separation, we computed the power spectrum of the velocity signal from hot-wire data, as shown in Figure 14. The inertial subrange can be identified, as characterized by the $-5/3$ law, with a span of around two decades. Evidently, the integral length scales and the small-scale motions belong to frequency bands clearly separated from each others.

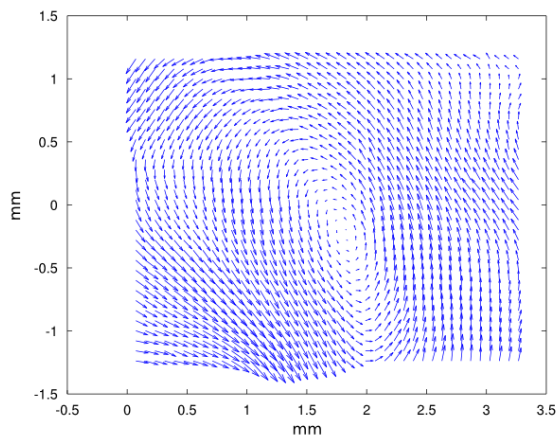


Figure 6: .

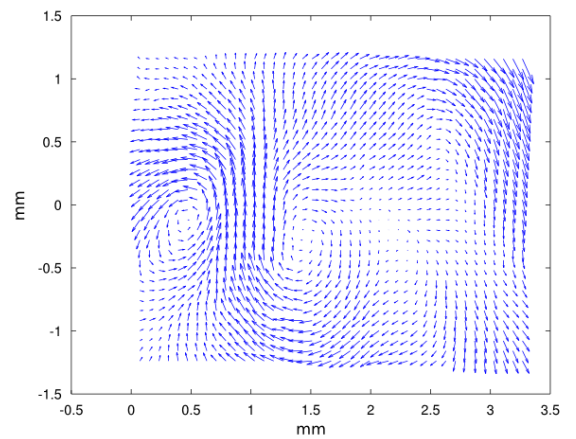


Figure 7:

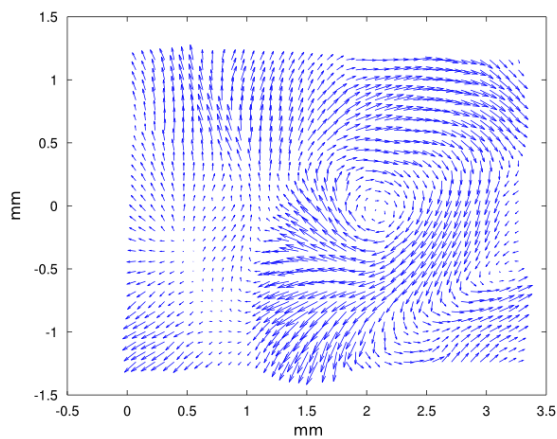


Figure 8:

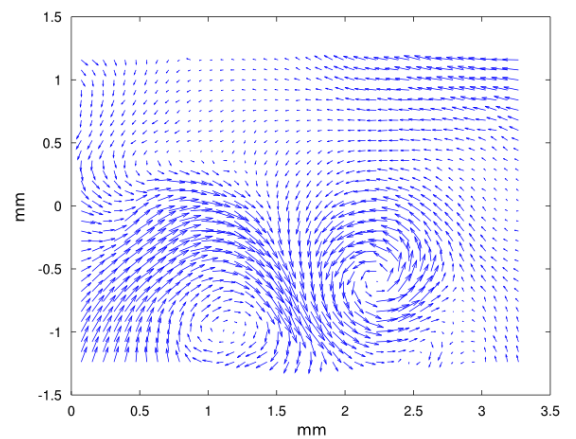


Figure 9:

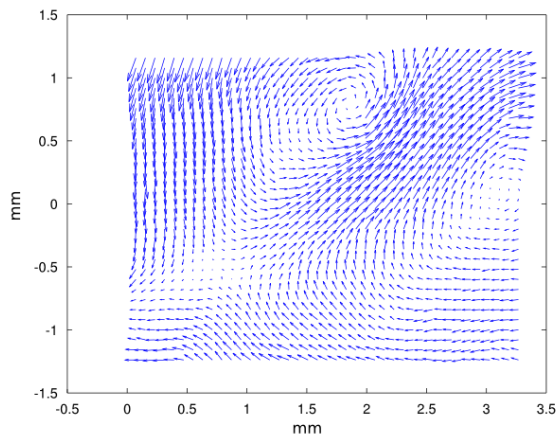


Figure 10:

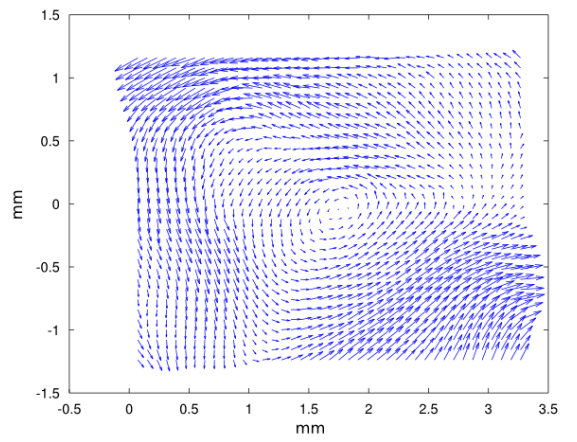


Figure 11:

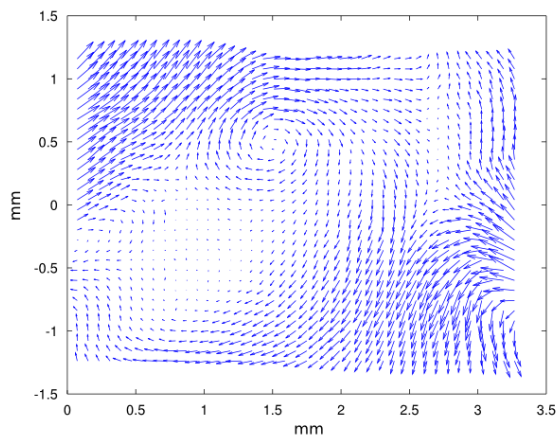


Figure 12:

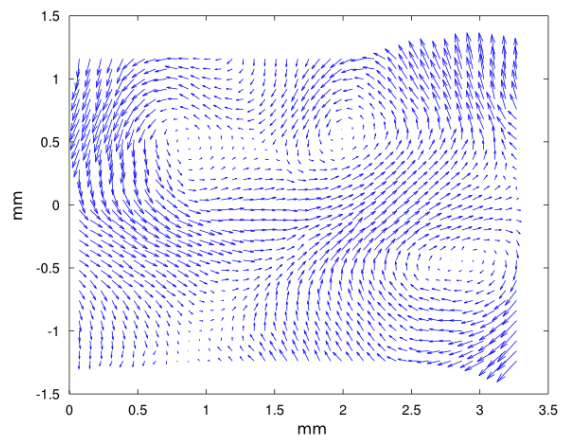


Figure 13:

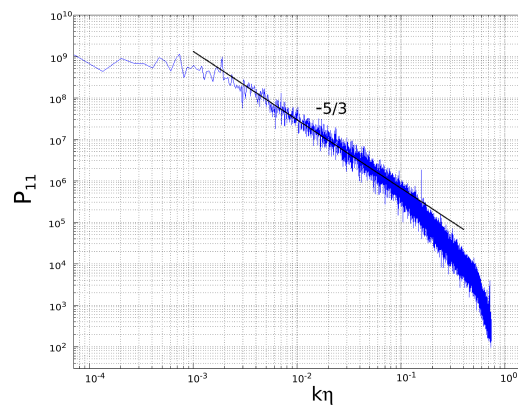


Figure 14: Power spectrum of the hot-wire signal taken at the jet centerline ($x/D = 70$)

CONCLUSIONS

In the present work, the small scale structures in the turbulent region of a high Reynolds number air jet were investigated with a long-range μ PIV system. The turbulence of the flow was characterized through a hot-wire analysis, which allowed to design of the μ PIV experiment. The main critical aspects in the implementation of the measurement technique, such as the low seeding concentration and the illumination of out-of-focus particles, were successfully solved. μ PIV measurements were acquired in proximity to the centerline, at the location of 70 diameters downstream, where the Kolmogorov length scale was estimated to be around 60 μ m. Typically, the fine scale motions have the tendency to organize themselves in worm-shaped structures, with a diameter scaling with the Kolmogorov length scale. A resolution in the velocity data of 80 μ m, obtained with an interrogation window size of 64 x 64 pixel, resulted adequate to capture the dissipative vortices within the flow. Additionally, with such an interrogation field size, the number of good vectors was higher than 94%. Eventually, the main turbulent statistics, computed on both PIV and hot-wire results, matched remarkably well, thus validating the experiment.

ACKNOWLEDGEMENTS

The authors would like to acknowledge Edwin Overmars and Simon Toet for their precious work, assistance, and help.

REFERENCES

- [1] Siggia ED "Numerical study of small-scale intermittency in three dimensional turbulence", J. Fluid Mech., 107 (1981), pp.375-406.
- [2] Jimenez J, Wray AA, Saffman PG, and Rogallo RS "The structure of intense vorticity in isotropic turbulence.", J. Fluid Mech., 255 (1993), pp.65-90.
- [3] Ganapathisubramani B, Lakshminarasimhan K, and Clemens NT "Investigation of three-dimensional structure of fine scales in a turbulent jet by using cinematographic stereoscopic particle image velocimetry.", J. Fluid Mech., 598 (2008), pp.141175.
- [4] Lindken R, Di Silvestro F, Westerweel J, Nieuwstadt FTM "Turbulence measurements with μ -PIV in large-scale pipe flows.", In: Proceedings of the 11th international symposium on application of laser technology to fluid mechanics, July 8-11 2012, Lisbon, Portugal.
- [5] Kähler CJ, Scholz U, and Ortmanns J "Wall-shear-stress and near-wall turbulence measurements up to single pixel resolution by means of long-distance micro-PIV.", Exp. Fluids, 41 (2006), pp.327-341.
- [6] Raffel M, Favier D, Berton E, Rondot C, Nsimba M, and Geissler W "Micro-PIV and ELDV wind tunnel investigations of the laminar separation bubble above a helicopter blade tip.", Meas. Sci. Technol., 17 (2006), pp.1652-1658.
- [7] Fiscaletti D, Elsinga GE, Ganapathisubramani B, Westerweel J "Amplitude and frequency modulation of the small scales in a turbulent jet.", submitted in: Proceedings of the 8th international symposium on turbulence and shear flow phenomena, August 28-30 2013, Poitiers, France.
- [8] Panchapakesan NR, and Lumley JL "Turbulence measurements in axisymmetric jets of air and helium. Part 1. Air Jet.", J. Fluid Mech., 246 (1993), pp.197-223.
- [9] Pope SB "Turbulent Flows." Cambridge University Press (2000).
- [10] Slot HJ, Moore P, Delfos R, and Boersma BJ "Experiments on the flow field and acoustic properties of a Mach number 0.75 turbulent air jet at a low Reynolds number.", Flow Turbulence Combust., 83 (2009), pp.587-611.
- [11] Adrian RJ, Westerweel J "Particle Image Velocimetry", Cambridge University Press, 2011.